

## Perception Range Prediction for IR Pilot Sight

Weiss, Robert  
 FGAN-FOM  
 Gutleuthausstr. 1, 76275 Ettlingen

### 1 INTRODUCTION

The new helicopters of the Bundeswehr, the UH Tiger and the NH-90, are equipped with a far-infrared Pilot Sight Unit (PSU). This sensor is used for both navigation and obstacle avoidance. At the beginning of our project, there was no established procedure to predict the IR viewing range under given weather conditions. Aviation safety guidelines, however, require a pre-flight assessment of prevalent viewing conditions for a given sensor. A high priority project was started by the German Office of Defense Technology and Procurement (BWB) where our institute cooperated with the Geophysical Institute of the Bundeswehr (AGeoBw), the General of Army Aviation (GenHFlg) and the Bundeswehr Technical Centers WTD 61 and WTD 91. The software package IRNAV, which resulted from this project, is in experimental use by the Bundeswehr since March 2007.

A direct generalization of the visibility concept as used for visual range is not possible; this is mostly due to the fact that the actual temperature of an object or background does not only depend on the current weather conditions but also those of the recent past. Depending on the material composition of this object, the reaction time to changing weather can be substantial. A tree, for example, will store residual heat for a much longer time after sunset than a metal tower. All this leads to a situation where one type of object will be clearly visible with an IR sensor while another one vanishes completely as its temperature approaches that of the background. We thus decided that perception range prediction for IR pilot sight units could not result in a single number as is the case for visual spectrum sensors. Instead, the perceptibility of objects relevant for navigation (e.g. roads, railroad tracks, houses) and obstacle avoidance (e.g. trees, towers) in front of typical backgrounds should be calculated individually and communicated to the pilots. In order to arrive at a reliable prediction of such ranges the following steps must be taken:

- Weather history recording and weather forecast
- Temperature variation modeling for object and background
- Perception range modeling and prediction

Weather data and forecasts are available at all airports and do not pose a problem; it is necessary, however, to also record diffuse and direct irradiation, since its history and forecasted values are needed for object/background temperature modeling. This step is carried out by the F-TOM [1] software package also developed at FGAN-FOM. This package uses a long time series of measured weather and object temperature data to derive fitting coefficients on a model that allows for rapid calculation of predicted (mean) object temperatures when supplied with recent weather data. The year-long (5 minute resolution) time series of data used for fitting in the context of the IRNAV project was recorded at WTD 61 and WTD 91. Along with a weather station, both thermistors in the objects and an IR camera were used for the measurements.

The temperature predictions by F-TOM are generally in good agreement with the actual temperatures of the objects (see Figure 1).

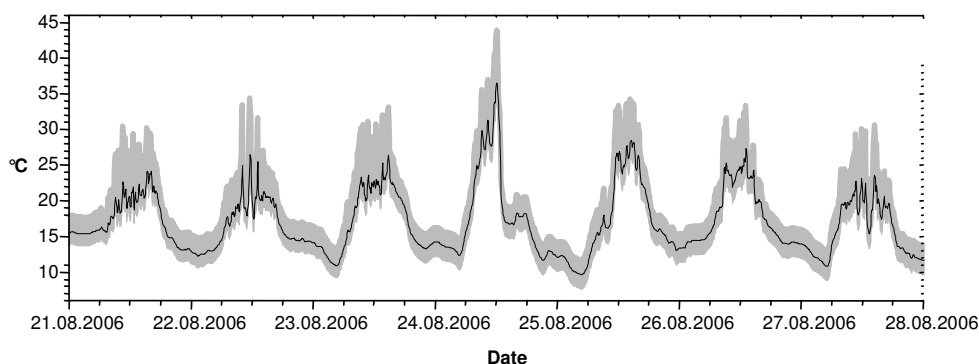


Figure 1. Object temperature prediction band (shaded) as derived from weather data for a lattice mast. Actual temperature (solid line).

With temperatures for object and background given, the perception ranges remain to be determined. In the context of our work, the task was target recognition, meaning the class of object (e.g. tree, tower) should be determined. Usually, Johnson criteria are a powerful tool to predict ranges for this kind of problem. For tanks and other military targets the necessary numbers of line pairs are readily available; unfortunately, this is not the case for objects relevant for navigation and obstacle avoidance. We thus had the choice to either derive the necessary Johnson criteria from observer experiments, or, since the number of objects and backgrounds was limited, to use synthetic PSU images of the relevant object/background combinations. The decision was taken to use the latter approach since we also suspected a significant dependence of perception ranges on object and background clutter, i.e. small-scale residual variations of the mean object/background temperature. Section 2 describes the derivation of perception models from observer experiments, while Section 3 deals with the review of these models by flight experiments.

## 2 PILOT IR SIGHT PERCEPTION MODELS

As mentioned above, we chose the approach to use synthetic PSU images to derive suitable perception models for the given problem. An obvious drawback of this is that the results thus obtained cannot be readily generalized to other sensor models. It will be seen, however, that we identified clutter as an important factor in actually achievable ranges, a result that could not have been found from Johnson criteria.

### 2.1 Objects and Backgrounds

The first important task was to identify objects that are a possible hazard to helicopters flying close to the ground; then, the relevant backgrounds for a central European environment had to be defined.

The types of objects selected as critical were cables, houses, lattice masts, towers, and trees (both foliate and defoliate), the backgrounds were farmland, forest, grassland, sky, and snow. Several realizations of each of the object and background types were used. In the following, a specific background or object (e.g. Tower of Type A) will be called an *instance* of an object or background *category* (e.g. Tower). Our aim was to derive perception models for category combinations which were to be derived by averaging over instance combinations of the given object/background category.

### 2.2 Image Synthesis

The images used for observer experiments are created by combining, after appropriate scaling, one object instance with a background instance. For this combination the following parameters can be varied for an individual combination:

- Object mean temperature  $T_{obj}$  and temperature standard deviation  $\sigma_{T,obj}$  (object clutter)
- Background mean temperature  $T_{back}$  and temperature standard deviation  $\sigma_{T,back}$  (background clutter); both background mean temperature and clutter are defined inside a rectangular region immediately surrounding the embedded object
- Viewing distance  $D$
- Object scaling

With the exception of very low temperatures, the visibility of an IR object in front of a background is only weakly dependent on absolute temperatures and strongly determined by the object-background temperature difference  $\Delta T = |T_{obj} - T_{back}|$ , which was thus used as a modeling parameter instead of the individual object/background temperatures along with object clutter  $\sigma_{T,obj}$ , background clutter  $\sigma_{T,back}$ , and the viewing distance  $D$ .

Combinations of all the object and background instances were created for different viewing distances in steps of 100 m. Since the most critical situations occur with low object-background temperature differences, images were generated for  $\Delta T = 0.0$  K, 0.25 K, 0.5 K, and 1.0 K. The object and background clutters were set to 0.25 K, 0.5 K, and 0.75 K simultaneously for each temperature difference, as the introduction of different clutter values for background and object, with the resulting number of possible combinations, would have rendered the sample size unmanageable.

All images were subjected to an IR imaging simulation using the software package PCSitoS [2] that recreates the whole imaging process of the UH Tiger/NH-90 IR sensor and PSU, from optics, photon noise, fixed pattern noise, video processing to display characteristics and spatial/temporal integration effects by the human eye. After this step, the distance sequence was reduced from 20 to 7 images by selecting the range of distances where recognition of the objects by the observer experiment subjects was deemed most likely. Figure 2 shows such a sequence for the instance combination *Tower Type C/Forest Type B* for  $\Delta T = 1$  K and  $\sigma_{T,obj} = \sigma_{T,back} = 0.5$  K.

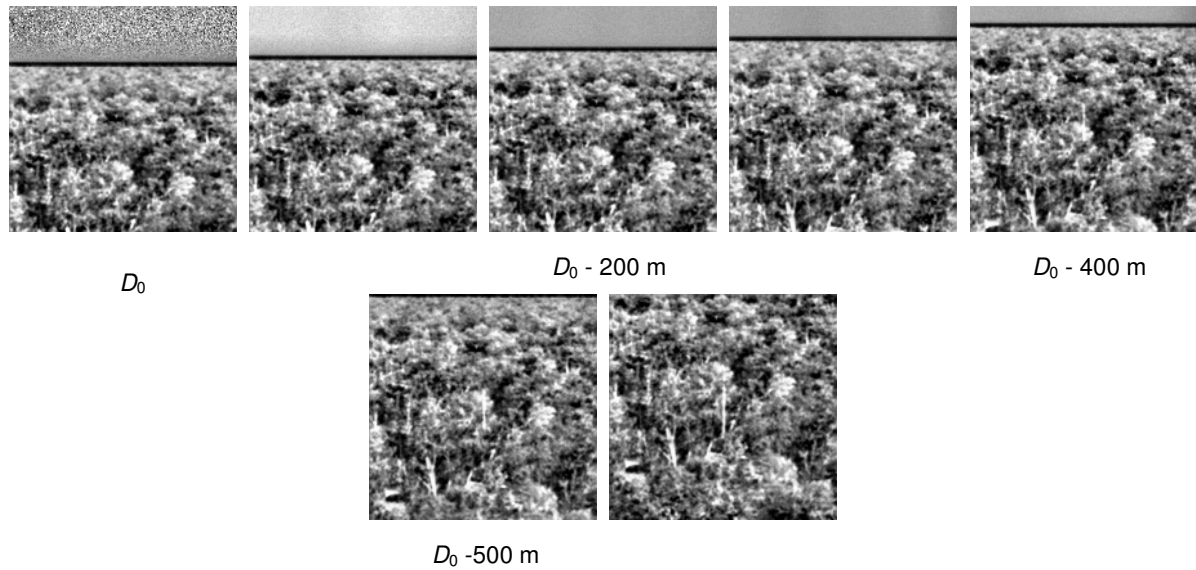


Figure 2. Final image sequence as showed during the observer experiments, where  $D_0$  is the starting distance. Object/Background combination was Tower Type C/Forest Type B; temperature difference was 1 K, clutter (in both object and background) 0.5 K

### 2.3 Observer Experiment Results

All of 812 image sequences generated by the process described in Section 2.2 were shown to students of the German Army Aviation School in Bückeburg and Celle during a two week measurement campaign in October 2006. There were between 12 and 24 observers available for each sequence; repetitive observation by the same experimental subject was mostly avoided.

The observer experiment was of the forced-choice type, i.e. an observer had the choice to answer “no object present”, “object present but category not recognized”, or to name the perceived object category by pressing buttons on a customized keyboard. The images of a sequence were shown consecutively with decreasing distance and a 4 second answer time. Failure to answer by the observer was classified as “no object present”.

The cumulative correct answers with decreasing distance to the specific object/background combinations were collected and grouped according to mean temperature difference and clutter. Finally, an error function was fitted to these results with the following additional constraints:

- Recognition probability at 0 m distance 100%,
- Recognition probability at 5000 m distance 0%.

Generally, the fit quality was very high; a few temperature difference/clutter combinations had to be excluded, however, due to very poor results (mostly superposition of two error functions with different mean values, which probably resulted from training effects of some groups of observers). The 50% recognition threshold probability distances in general varied by some tens of meters, while the variances of the fitted error functions generally were on the order of 100 m to 200 m.

### 2.4 The perception model

In order to establish the connection between predicted and/or measured temperature differences and the 50% recognition probability distance, the results of the observer experiments for a given object/background category must be fitted by a suitable function. It turned out that mean temperature difference alone was not a good predictor of actual recognizability, since the mean recognition distances varied strongly with clutter (see Figure 3).

To overcome this limitation, clearly a better modeling parameter for the given temperature/clutter situation is necessary. This can be accomplished by using the *Signal-to-Clutter Ratio* (SCR), defined as

$$SCR = \frac{\sqrt{\Delta T^2 + \sigma_{T,obj}^2}}{\sigma_{T,back}}, \quad (1)$$

which increases with increasing inhomogeneity of the mean object temperature as well as increasing homogeneity of the background. Note that in principle the temperature difference and clutter values would have to be replaced by their respective effective temperatures due to atmospheric extinction. Since the background clutter value, however,

refers to the immediate surrounding of the object, the effect of atmospheric extinction is the same in numerator and denominator which thus cancels in the definition of the SCR. Of course, atmospheric extinction still has an effect on the mean recognition distance; this is due to the attenuation of overall signal strength which increases photon noise. To account for this, an additional extinction factor is introduced into Equation (1)

$$SCR = \frac{\sqrt{\Delta T^2 + \sigma_{T,obj}^2}}{\sigma_{T,back}} e^{-\lambda D} \quad (2)$$

where  $\lambda$  is the atmospheric extinction coefficient, and  $D$  the distance from the observer to the object.

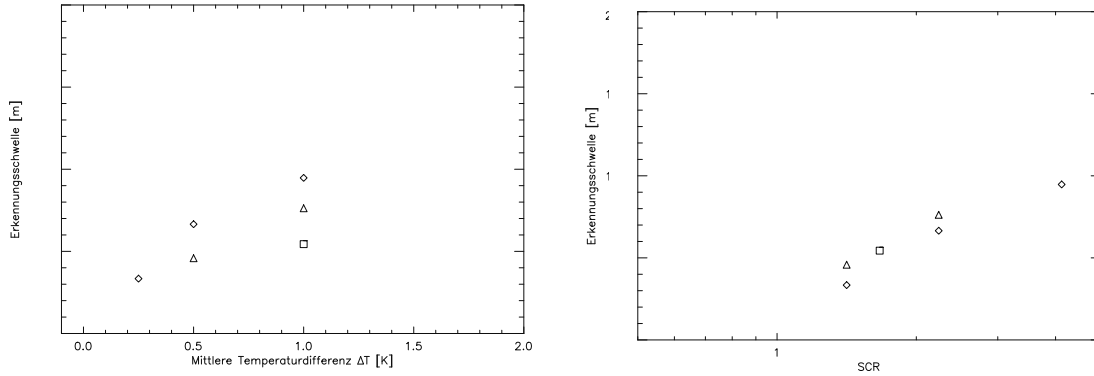


Figure 3. Total results for the instance combination Tower Type C/Forest Type C. Left: mean recognition distance dependence on mean temperature difference. Right: mean recognition distance dependence on Signal-to-Clutter ratio. Clutter denoted by symbols: 0.25 K (diamonds), 0.5 K (triangles), 0.75 K (squares).

For the fitting procedure,  $\lambda$  was set to 0. In general, it turned out that the observer data could be well approximated by a two-parameter log-linear fit, at least in the domain of SCRs that were used for the experiment:

$$D = a_1 \ln SCR + a_2 \quad (3)$$

where  $a_1$  and  $a_2$  are the fitting parameters, and  $D$  is the mean recognition distance. To obtain a perception model, all mean recognition for a given SCR of an object/background category were averaged and Equation (3) fitted to it.

With the fitting parameters known, and temperature difference, clutter values and atmospheric extinction taken from temperature and weather predictions respectively, an estimate of the mean recognition distance is then obtained from putting equation (2) into equation (3) and solving for  $D$ :

$$D = \frac{1}{1 + a_1 \lambda} \left[ \frac{a_1}{2} \ln \left( \frac{\Delta T^2 + \sigma_{T,obj}^2}{\sigma_{T,back}^2} \right) + a_2 \right] \quad (4)$$

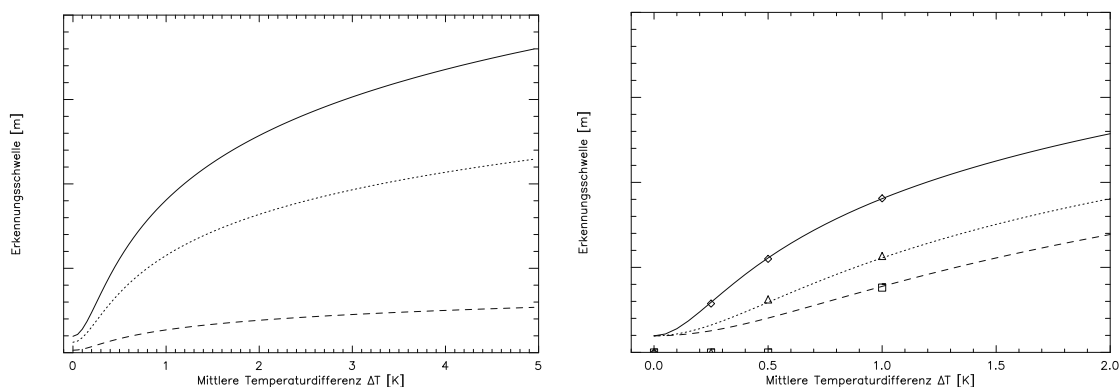


Figure 4. Mean recognition distance predictions for the Tower/Forest perception model in dependence on mean temperature difference. Effect of atmospheric extinction (left): with  $0 \text{ km}^{-1}$  (solid),  $10^{-3} \text{ km}^{-1}$  (dotted),  $10^{-1} \text{ km}^{-1}$  (dashed) on a model with  $\sigma_{T,obj} = \sigma_{T,back} = 0.25 \text{ K}$ . Effect of object/background clutter (right):  $\sigma_{T,obj} = \sigma_{T,back} = 0.25 \text{ K}$  (solid, diamonds),  $\sigma_{T,obj} = \sigma_{T,back} = 0.5 \text{ K}$  (dotted, triangles),  $\sigma_{T,obj} = \sigma_{T,back} = 0.75 \text{ K}$  (dashed, squares).

Figure 4 shows mean recognition range predictions for the Tower/Forest category perception model in dependence of mean temperature difference for different values of atmospheric extinction and object/background clutter.

Models like these were produced for all object/background category combinations. While most showed acceptable variation in the fitting parameter values, some objects and backgrounds proved to be too diverse to be fitted into a single category. This problem proved especially persistent when combining lattice masts with different kinds of forests (coniferous/deciduous/mixed forest), possibly due to the similarity in shape and appearance of needle leaf trees and lattice masts. Unfortunately, the data available so far is not sufficient for a conclusive decision, but future refinements of the model will probably include a further splitting of categories.

### 3 PERCEPTION MODEL VALIDATION

The perception models were subjected to a validation campaign from January to September 2007, using the MAT (mission equipment test helicopter) platform operated by WTD 61 in Manching, Germany. This helicopter is a modified Bell UH-1D that can be equipped with different sensors and carry extensive experimental equipment. In our case the complete UH Tiger IR camera and PSU was installed.

The pilots were asked to follow a flight path that included approaches to the relevant object and background combinations; individual recognition distances were recorded by a marker both on the recorded flight videos and a GPS tracking device when the pilots hit a button on their flight control stick.

Between 12 and 20 approaches were made for each of the present object/background combinations. These approaches included flights during day- and nighttime as well as under adverse visual weather conditions, thus covering a sufficient range of temperature differences.

At some of the approach locations, simultaneous measurements with a calibrated IR camera were carried out at ground level, in order to obtain the ground truth values for temperature difference and clutter independent of weather forecasts and temperature predictions.

The temperature data extracted from the ground images was used to calculate recognition range predictions both for a fixed object and background clutter value of 0.5 K and using the actually measured clutter. The predicted values were then compared to the recognition ranges as reported by the pilots. From the deviations, a distribution of (actual) recognition ranges could be constructed which could then be compared to the expected distribution as calculated from the perception models.

Figure 5 shows a comparison between prediction and observation for the Lattice Mast/Farmland category. As can be seen, the mean recognition distance is underestimated by about 250 m when using the uniform clutter of 0.5 K, a deviation that was highly significant when using a T-test. If the actual clutter is used, however, the observed mean recognition distance differs from the expected one by only 70 m, and there is no statistically significant deviation of the means and variances of the two distributions. This clearly shows that using the SCR improves the quality of the prediction under real conditions, too.

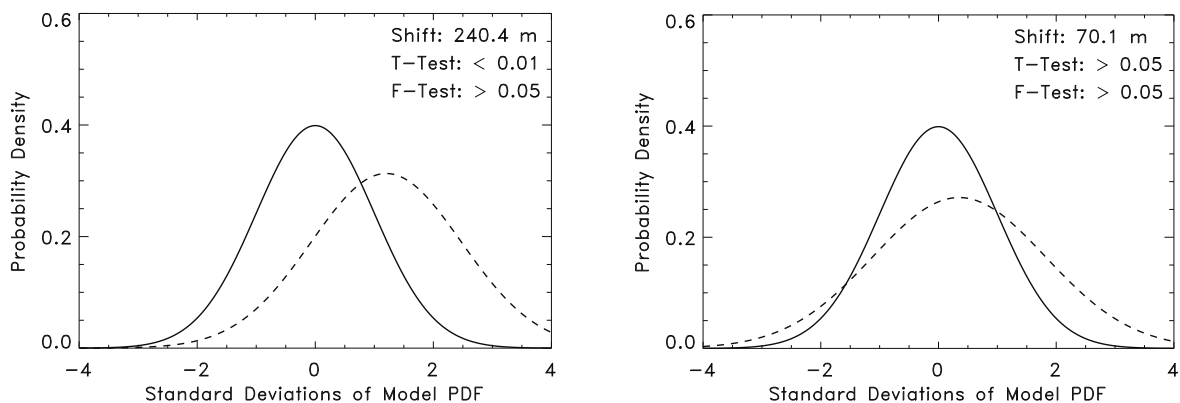


Figure 5. Comparison between the expected (solid) and observed (slashed) distributions of recognition distances using uniform clutter of 0.5 K (left) and measured clutter (right).

It should be noted however, that using the definition of SCR as denoted in Equation (2) fails when the background clutter is much lower than 0.2 K; in these cases the predicted recognition range is strongly overestimated. This limitation can be overcome by using the sensor NETD as a lower limit for both object and background clutter.

There are further limitations to the SCR approach as can be, e.g., from an approach to a house on grassland.

Since clutter is simply defined as the standard deviation from mean temperature, object clutter for houses tends to be very large due to the high temperature differences between the different building materials like shingles, bricks, paint etc. The idea behind using clutter, however, is to regard it as high (spatial) frequency structured noise, which is clearly violated in the case of a house. The use of the very high measured clutter lead to a significant overestimation of the achievable recognition ranges for houses.

This situation could be ameliorated by using uniform clutter of 0.5 K in the object and the measured clutter for the background. Then, there was good agreement between predicted and actual recognition ranges. The variances of all of the observed recognition range distribution still was significantly higher than that of the expected one for houses. A possible explanation might be the changing viewing perspectives during approach. The observer experiments mostly used frontal views of houses, while the validation flights took place at an altitude of about 300 ft above ground level; leading to a stronger contribution of the roof to the perception of the house. This question will have to be addressed in future observer experiments.

#### 4 CONCLUSIONS AND FUTURE WORK

We presented results of a large-scale observer experiment carried out to obtain reliable predictions for the mean recognition ranges of obstacles and navigation cues using a infrared pilot sight unit. As could be seen, a single temperature difference between an object and its background is not sufficient to arrive at a conclusive perception distance estimate. The temperature discrimination abilities of modern IR sensors require small temperature variations in both object and background to be taken into account. This can be accomplished by using a Signal-to-Clutter ratio (SCR).

With the SCR as an independent parameter, a simple log-linear perception model successfully accounts for mean recognition ranges of a variety of object/background combinations. The validity of the perception models deduced from the observer experiments has been assessed by experimental flights using the IR pilot sight unit.

During these validation flights, some limitations of the SCR approach became apparent; very low background clutter can lead to a significant overestimation of actual recognition distances, while large scale, low spatial frequency temperature variations in objects can render the object clutter approach ineffective. These limitations can be overcome by setting a lower limit for background clutter and using a fixed clutter value for complex objects.

Future refinements of the models will include a sub-categorization where certain objects or background categories proved to be broad for satisfactory model fits, and a further improvement of the SCR approach, especially on the question of atmospheric extinction.

Additionally, the observer experiments provided a wealth of data with well-defined object and background statistical properties which might be used to explore correlations between object/background structure and appearance and expected recognition range performance for future sensors.

#### 5 REFERENCES

1. A. Malaplate, P. Grossmann, F. Schwenger, "CUBI: a test body for thermal object model validation," in *Infrared Imaging Systems: Design, Analysis, Modeling, and Testing XVIII*, G. C. Holst, ed., Proc. SPIE 6543, pp. 5-7, 2007.
2. E. Repasi, H.-J. Greif, "Generation of dynamic IR scenes for ground-based systems and missile applications", in *Infrared Technology and Applications XXIV*, B.F. Andresen, M. Strojnik, Eds., Proc. SPIE 3436, pp. 458-464, 1998.
3. D. Clement, R. Ebert, P. Großmann, E. Repasi, R. Rexer, G. Ritt, P. Schlippe, R. Weiss, W. Wittenstein, "Conception and validation of methods to forecast infrared visibility", Technical Report **FOM 2007/03**, FGAN-FOM, Ettlingen, Germany, 2007
4. P. Großmann, R. Rexer, G. Ritt, P. Schlippe, R. Weiss, "Optimization of methods to forecast infrared visibility for the flight control of helicopters", Technical Report **FOM 2007/19**, FGAN-FOM, Ettlingen, Germany